

Once a catalog of resonance positions associated with each phase has been established, this work has demonstrated that MAS-NMR (particularly  $^{29}\text{Si}$ ) is a powerful technique for examining ceramic phases. It can be used simply as a "finger-printing" technique to identify phases in complex phase mixtures, some of which were missed by conventional XRD analysis. MAS-NMR will give most advantage when mixtures of crystalline and glassy

phases occur, and this is currently being investigated. MAS-NMR is an expanding field which will be increasingly used to probe ceramic systems.

**Acknowledgment.** We thank the SERC for support and a studentship (M.E.S.). We also thank Professor R. K. Harris for communication of his work prior to publication.

## Biosynthetic Studies Using $^{13}\text{C}$ -COSY: The *Klebsiella* K3 Serotype Polysaccharide

David N. M. Jones and Jeremy K. M. Sanders\*

Contribution from the University Chemical Laboratory, Lensfield Road, Cambridge, CB2 1EW U.K. Received December 29, 1988

**Abstract:** The biosynthesis of the *Klebsiella* K3 serotype polysaccharide has been elucidated by  $^{13}\text{C}$  NMR spectroscopy of intact cultures under physiological conditions. Biosynthetic enrichment with  $[1-^{13}\text{C}]$ glucose suggested that the major biosynthetic pathway involved direct incorporation of the hexose moiety into the polysaccharide. A detailed analysis of the isotopomer distribution in the cross peaks of a phase-sensitive  $^{13}\text{C}$ -COSY spectrum of polysaccharide biosynthetically labeled with  $[\text{U}-^{13}\text{C}_6]$ glucose revealed that approximately 30% of the glucose was catabolized prior to incorporation. Detailed analysis of the cross peaks in the phase-sensitive spectrum provided strong evidence that catabolism proceeds via the phosphogluconate pathway, a conclusion confirmed by the results of biosynthetic enrichment with  $[2-^{13}\text{C}]$ glucose.

$^{13}\text{C}$  labeling for NMR spectroscopy has found widespread application in the elucidation of biosynthetic pathways in many organisms. However, the use of one-dimensional  $^{13}\text{C}$  NMR spectroscopy is often limited in systems involving complex molecules. This complexity leads to crowded, overlapped spectra that are difficult to interpret. Recently Beale et al.<sup>1</sup> have developed triple-quantum-filtered INADEQUATE techniques to study the direct incorporation of  $[\text{U}-^{13}\text{C}_3]$ glycerol. We now show how  $^{13}\text{C}$ -COSY spectroscopy can be used to obtain simultaneously information about intact and non-intact incorporation of  $^{13}\text{C}$ -labeled precursors. In particular, we point out that the detailed information about the metabolic pathways involved in biosynthesis is contained in the isotopomer distributions which can be extracted from the multiplet patterns within the cross peaks of the COSY spectrum.

The appearance of cross-peak patterns in phase-sensitive COSY spectra is well understood. If A, M, and X are mutually coupled, then the cross peak between A and M has  $J_{\text{AM}}$  as the active coupling and  $J_{\text{AX}}$  or  $J_{\text{MX}}$  as the passive couplings. Lines separated by the active coupling appear antiphase, while those separated by a passive coupling appear in-phase. In  $^1\text{H}$ -COSY spectra the observed nucleus is 100% abundant, with the result that all spins are coupled to all other adjacent spins and the cross peaks contain the full multiplets in both dimensions. Consequently there is no difference between the type of information available from the cross peaks in either dimension. This type of analysis is routine for  $^1\text{H}$ -COSY spectra, including those of oligosaccharides.<sup>2</sup>

$^{13}\text{C}$ -COSY spectra of biosynthetically labeled molecules are dramatically different, due to the appearance of additional multiplets within the cross peaks. The observed cross peaks are a combination of superimposed responses from molecules with different patterns of  $^{13}\text{C}$  labeling. The presence of these additional components is attributable to substrate catabolism, which results in the loss of  $^{13}\text{C}$  label at various sites. The appearance of these additional components can be used to analyze the substrate metabolism by exploiting the information provided by the active and passive coupling contributions to each cross peak. In the following discussion a shorthand notation for distinguishing between the

cross peaks is adopted: the C-4, C-5 cross peak observed at  $\delta$  C-4 in  $f_2$  is represented as  $\text{C}_{45}^4$  with the corresponding cross peak at  $\delta$  C-5 being represented as  $\text{C}_{45}^5$ .

The metabolic information available from COSY spectroscopy is illustrated for the *Klebsiella* K3 serotype polysaccharide that was biosynthetically labeled with specifically labeled glucose and universally labeled glucose as the carbon substrates. Labeling with  $[1-^{13}\text{C}]$ glucose showed that the major biosynthetic pathway for the polysaccharide incorporated the hexose moiety intact, while labeling with  $[\text{U}-^{13}\text{C}_6]$ glucose allowed us to acquire a  $^{13}\text{C}$ -COSY spectrum and subsequently completely assign the one-dimensional  $^{13}\text{C}$  NMR spectrum.<sup>3</sup> We show here that detailed analysis of the phase-sensitive cross peaks in the  $^{13}\text{C}$ -COSY spectrum provides a powerful method for elucidating isotope distribution patterns and that, in this case, the pattern is consistent with a significant percentage of the glucose being catabolized through the phosphogluconate pathway prior to incorporation into the polysaccharide. These conclusions were confirmed by biosynthetically labeling the polysaccharide with  $[2-^{13}\text{C}]$ glucose and observing the predicted distribution of  $^{13}\text{C}$  label in the resulting one-dimensional spectrum.

### Results

The primary sequence (1) of the *Klebsiella* K3 serotype polysaccharide has recently been determined by Dutton and co-workers.<sup>4</sup> An initial spectrum was recorded at a low level of uniform labeling by using  $[\text{U}-14\% -^{13}\text{C}_6]$ glucose (Figure 1a) and was found to be consistent with spectra recorded at the natural abundance level. The spectrum can be divided into four distinct regions: the carboxyl region (170–180 ppm), not shown but containing two resonances; the anomeric region (95–105 ppm), containing five well-resolved anomeric resonances; the ring region (60–80 ppm), containing 24 resonances with the lower field extreme corresponding to the glycosidically linked carbons and the

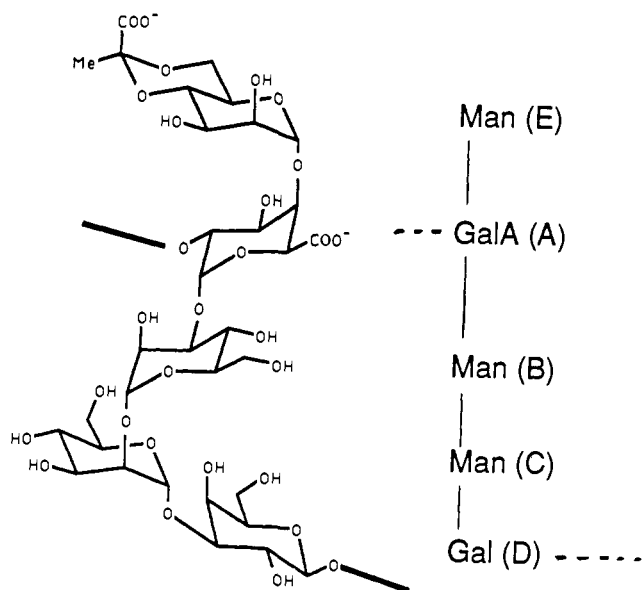
(1) Beale, J. M.; Cottrell, C. E.; Keller, P. J.; Floss, H. G. *J. Magn. Reson.* **1987**, *72*, 574–578.

(2) Berman, E. *Eur. J. Biochem.* **1987**, *165*, 385–391.

(3) Jones, D. N. M.; Sanders, J. K. M. *J. Chem. Soc., Chem. Commun.* **1989**, 167–169.

(4) Dutton, G. G. S.; Parolis, H.; Joseleau, J.-P.; Marais, M.-F. *Carbohydr. Res.* **1986**, *149*, 411–423.

\* Author to whom correspondence should be addressed.



1

higher field extreme to the C-6 methylene groups; the signal at 26 ppm, which corresponds to the methyl of the pyruvate ketal in an equatorial configuration.<sup>5</sup>

**Labeling with  $[1-^{13}\text{C}]$ Glucose.** Before attempting to biosynthetically enrich the whole molecule with  $^{13}\text{C}$ , it was necessary to establish whether there is extensive substrate catabolism prior to polysaccharide biosynthesis. This was achieved by growing the bacteria on a medium containing a mixture of C-1 labeled glucose and unlabeled glucose, the final proportion of  $[1-^{13}\text{C}]$ glucose being approximately 20%. The resulting spectrum, which was obtained from an intact culture under physiological conditions (Figure 1b), has three notable features: (1) the intensity of the anomeric signals is substantially enhanced relative to the other signals in the spectrum; (2) the intensities of the anomeric signals relative to each other is essentially unchanged; (3) the intensities of the signals at 61.9 and 25.9 ppm are also slightly enhanced relative to those signals between 65 and 80 ppm. This suggested that the bulk of the substrate was being incorporated directly into the polysaccharide with a small proportion being catabolized prior to incorporation.

These observations can be explained by catabolism of glucose to pyruvate, which is used as a precursor for the biosynthesis of the hexose components of the polysaccharide. During glycolysis, C-1 and C-6, C-2 and C-5, and C-3 and C-4 of glucose become equivalent by conversion of dihydroxyacetone phosphate to glyceraldehyde-3-phosphate by triose phosphate isomerase. Hence some of the C-1 label is converted to a C-6 label, and this accounts for the observed enhanced intensities of the signals at 26 and 62 ppm. However, the extent of catabolism by this pathway appears to be low enough for biosynthetic enrichment of the whole molecule to be a realistic proposition.

**Labeling with  $[^{13}\text{C}_6]$ Glucose.** A sample of universally labeled polysaccharide was produced by growing the bacteria on a medium containing  $[^{13}\text{C}_6]$ glucose and unlabeled glucose, the overall proportion of labeled glucose again being 20%. The resulting one-dimensional spectrum is more complex than the natural abundance spectrum and does not readily permit analysis for biosynthetic or assignment information due to extensive overlap of signals. However, this sample was used to perform a phase-sensitive double-quantum-filtered COSY experiment<sup>6</sup> of the region 55–110

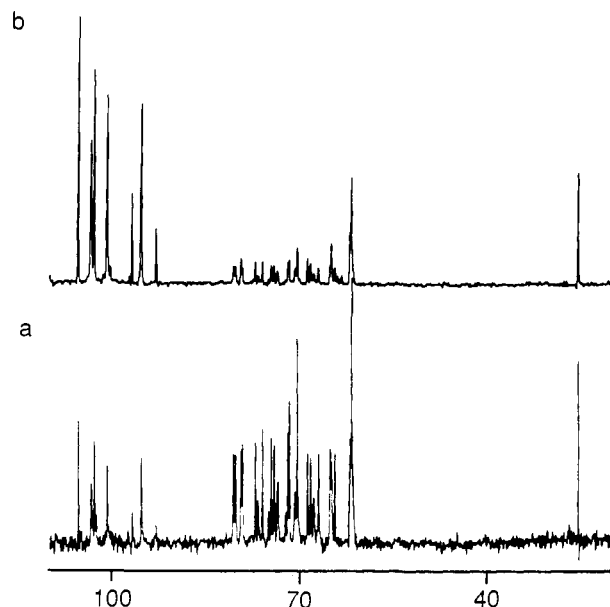


**Figure 1.** One-dimensional spectra of the *Klebsiella* K3 serotype polysaccharide obtained from cultures grown on (a) 10%  $[U-^{13}\text{C}_6]$ glucose, 20 000 transients, and (b) 20%  $[1-^{13}\text{C}]$ glucose, 3072 transients. In both cases the spectral width was 10 638 Hz with a total acquisition time of 0.77 s.

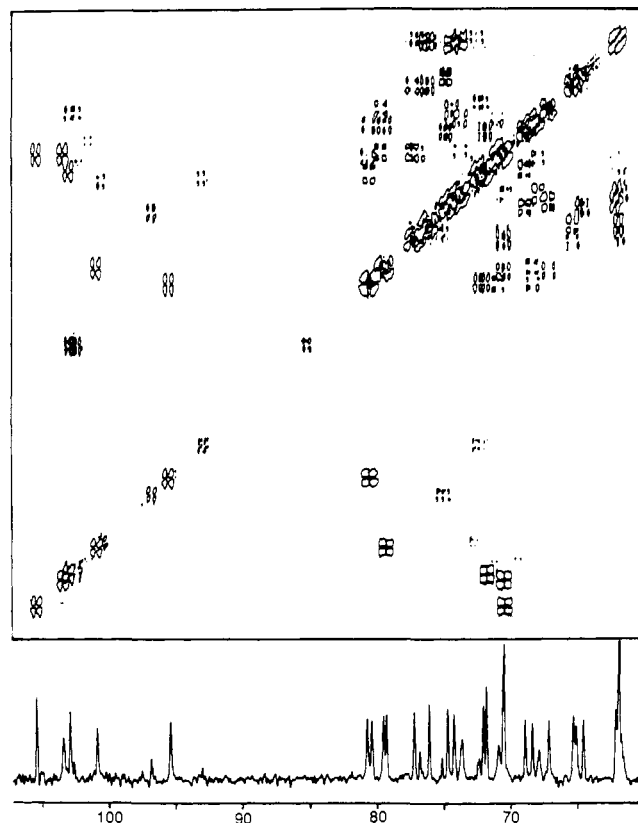


**Figure 2.** DQF-COSY spectrum of the region 55–110 ppm obtained from a culture of *Klebsiella* K3 grown on  $[U-^{13}\text{C}_6]$ glucose. The spectral width in both dimensions was 5494 Hz, giving an acquisition time of 0.4 s in the  $f_2$  dimension. In the  $f_1$  dimension,  $t_1$  was incremented in 256 equal steps to a maximum value of 0.023 s. 512 transients were acquired per  $t_1$  increment, and the data were zero filled to 512 points prior to Fourier transformation with mild Lorentzian to Gaussian apodization in both dimensions.

ppm. The resulting COSY spectrum (Figure 2) allowed complete assignment of the one-dimensional  $^{13}\text{C}$  NMR spectrum<sup>3</sup> (Table I). In the following discussion only cross sections taken parallel to  $f_2$  are discussed as the digital resolution in  $f_1$  is insufficient to

(5) Garegg, P. J.; Lindberg, B.; Kvarnström, I. *Carbohydr. Res.* **1979**, *77*, 71–78.

(6) Sanders, J. K. M.; Hunter, B. K. *Modern NMR Spectroscopy: A Guide For Chemists*, revised edition; Oxford University Press: Oxford, 1988; p 126.

**Table I.** Complete  $^{13}\text{C}$  NMR Assignments of the *Klebsiella* K3 Serotype Polysaccharide<sup>a</sup>

atom	$\alpha$ -GalA (A)	$\alpha$ -Man (B)	$\alpha$ -Man (C)	$\beta$ -Gal (D)	$\alpha$ -Man (E)	Pyr
C-1	100.8	103.3	95.8	105.4	102.8	176.2
C-2	79.3	70.5	80.4	70.5	71.8	102.7
C-3	68.5	79.6	71.0	77.6	68.9	25.9
C-4	80.2	67.2	68.0	65.4	74.7	
C-5	72.1	74.2	73.6	76.1	64.5	
C-6	175.5	62.1	61.9	61.9	65.1	

<sup>a</sup> Values are given relative to internal acetone ( $\delta$  31.07 ppm).

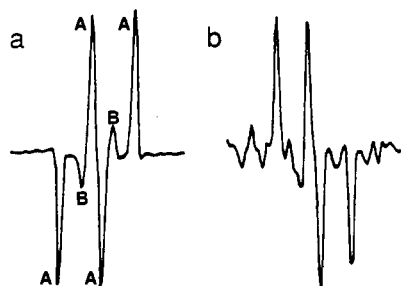


**Figure 3.** Cross sections from the correlations between the quaternary carbon of the pyruvate acetal and (a) the pyruvate methyl, the peaks labeled A arising from molecules with three coupled carbons and the peaks B from molecules with two coupled carbons, and (b) the pyruvate carboxyl.

resolve the fine structure of the cross-peak multiplets.

The first observation that we made is that there are two peaks aliased in the  $f_1$  dimension at  $\delta$  100.7 ppm in  $f_2$ . These peaks we have attributed to the methyl and carboxyl groups of the pyruvate acetal. The assignment of the cross peak is based on the size of the active coupling constants,  $J_{\text{C-C=O}}$  being much larger than the  $J_{\text{C-Me}}$ . In the cross peak at 85.2 ppm in  $f_1$  the active coupling is 46 Hz and the passive coupling is 62 Hz, these relationships being reversed for the cross peak at 67.2 ppm in  $f_1$  (Figure 3). Thus the methyl cross peak, with the passive carboxyl coupling, is aliased once at 85.2 ppm in the  $f_1$  dimension, inverting the relative phases of the multiplets, and consists of six lines (Figure 3a). The four intense lines labeled A can be attributed to molecules with all three carbons labeled with  $^{13}\text{C}$ , while the two weaker lines, B, to molecules with only two carbons labeled, the  $^{13}\text{C}$  label at the carboxyl having been lost. The other cross peak from the carboxyl, with the passive coupling to the methyl, is aliased twice at 67.2 ppm, thus reinverting the relative phases of the multiplets. This cross peak has only four lines (Figure 3b) in the multiplet, and hence we can deduce that all molecules retaining the carboxyl and the acetal carbon also retain the methyl carbon.

All the  $\text{C}_{12}^1$  cross peaks appear as clean antiphase doublets characteristic of two coupled nuclei (Figure 4). In contrast, the  $\text{C}_{12}^2$  cross peaks are more complex, containing a total of six lines. The pattern expected for a 100% labeled polymer would be a simple double doublet; this corresponds to the four lines labeled A. The doublet labeled B is an active coupling and therefore arises from molecules without a C-3 label. Thus we can infer that there is a proportion of molecules with C-1, C-2, and C-3 labeled and a proportion with C-1 and C-2 labeled but C-3 unlabeled.

The  $\text{C}_{23}^2$  cross peaks all show a simple double-doublet pattern showing that these arise from molecules where C-1, C-2, and C-3 are all labeled. From this we can say that all C-1, C-2, and C-3 units that have a  $^{13}\text{C}$  at C-2 and C-3 are incorporated intact. In contrast the  $\text{C}_{23}^3$  cross peaks all show a more complex pattern similar to that observed in the  $\text{C}_{12}^2$  cross peaks. The difference here is that  $J_{2,3}$  and  $J_{3,4}$  are almost identical, and the two central components of the double doublet, which are antiphase with respect to each other, cancel. The multiplet labeled A now arises from C-2, C-3, and C-4 labeled molecules, and the multiplet labeled B from molecules where C-2 and C-3 are labeled but C-4 is unlabeled.

The  $\text{C}_{34}^3$  cross peaks again exhibit the intricate multiplet pattern, those peaks labeled A arising from molecules labeled at C-2, C-3, and C-4, and the multiplet labeled B arising from molecules with

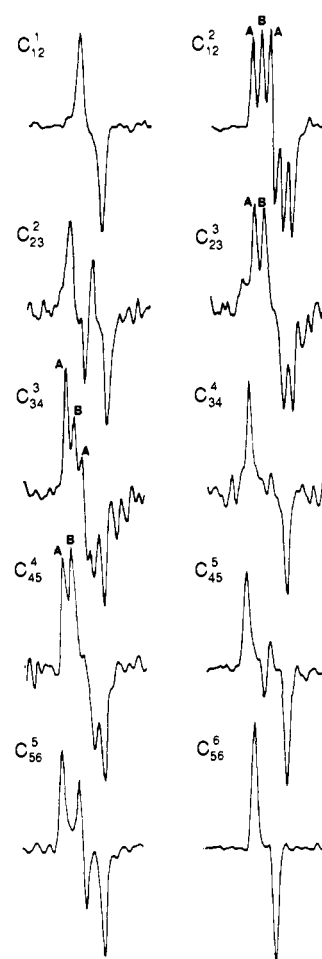


**Figure 4.** Representative cross sections extracted from the COSY correlations between carbons in the hexose rings of the *Klebsiella* K3 serotype polysaccharide. The multiplets from the cross peaks show the same patterns for all the hexose units, as illustrated, except for the  $\text{C}_{45}^4$  and  $\text{C}_{56}^5$  cross peak of the  $\alpha$ -galacturonic acid (A). The larger coupling to the carboxyl group distorts the appearance of the multiplets,<sup>3</sup> but the final analysis of the cross peaks is unchanged.

C-3 and C-4 labeled but not C-2. The  $\text{C}_{34}^4$  cross peak shows the clean double doublet, suggesting that where C-3 and C-4 are labeled C-5 is also labeled. This is in distinct contrast to C-2, where loss of label is readily observed. Initially we thought that the observed patterns were due to glucose catabolism through the citric acid cycle, as suggested by the labeling with  $[1-^{13}\text{C}]$ glucose. If this was the case then C-1 and C-6, C-2 and C-5, and C-3 and C-4 would become equivalent and we would expect to see the loss of labels reflected symmetrically in both halves of the hexose moieties. This is clearly not the case as we are observing preferential loss of label at C-2 and C-3 over C-5 and C-4, respectively. Further evidence for this differential loss of label is seen in  $\text{C}_{45}^4$  cross peaks, the multiplet pattern A, arising from molecules with C-3, C-4, and C-5 labeled and multiplet B, from other molecules with C-4 and C-5 labeled but C-3 unlabeled. The  $\text{C}_{45}^5$  cross peaks show no loss of label at C-6 and the  $\text{C}_{56}^5$  cross peaks no loss of label at C-4. The final set of cross peaks  $\text{C}_{56}^6$  show the doublet characteristic of two adjacent coupled nuclei.

**Table II.** Isotopomers Present in the *Klebsiella* K3 Serotype Polysaccharide, Inferred from Analysis of the Experimental Cross Peaks in Figure 4

cross peak	isotopomers
$\text{C}_{12}^1$	1*-2*-3-4-5-6
$\text{C}_{12}^2$	1*-2*-3-4-5-6, 1*-2*-3*-4-5-6
$\text{C}_{23}^2$	1*-2*-3*-4-5-6
$\text{C}_{23}^3$	1-2*-3*-4-5-6, 1-2*-3*-4*-5-6
$\text{C}_{34}^3$	1-2*-3*-4*-5-6, 1-2-3*-4*-5-6
$\text{C}_{34}^4$	1-2-3*-4*-5*-6
$\text{C}_{45}^4$	1-2-3*-4*-5*-6, 1-2-3-4*-5*-6
$\text{C}_{45}^5$	1-2-3-4*-5*-6*
$\text{C}_{56}^5$	1-2-3-4*-5*-6*
$\text{C}_{56}^6$	1-2-3-4-5*-6*

It is clear that the cross-peak multiplet patterns are a combination of superimposed responses from molecules with differing labeling patterns. A large percentage of three-carbon ( $\text{C}_3$ ) units is being incorporated intact, but there are a number of different isotopomers contributing to the spectrum. The different isotopomers that can be detected from the analysis of each of the cross peaks are given in Table II. Since each cross peak has a different "reading frame" of three nuclei (because we can observe only one-bond couplings) it is not possible to distinguish whether some of the inferred labeling patterns arise from the same or from different isotopomers. However, these cross peaks strongly indicate that the major catabolic pathway involved in the bacteria degrades the hexose unit into a two-carbon and a four-carbon unit before recombining them into hexose units for polysaccharide biosynthesis. These observations are consistent with catabolism via the phosphogluconate pathway.

The catabolism of carbohydrates in *Klebsiella* species has been the subject of many studies;<sup>7-13</sup> these have shown<sup>14,15</sup> that the phosphogluconate pathway is a major pathway for the catabolism of carbohydrates. The phosphogluconate pathway (also known as the pentose phosphate pathway or hexamono-phosphate shunt) is an alternative pathway to glycolysis for the oxidation of glucose. Perhaps more importantly this pathway is the primary source of NADPH, the major reducing power in biosynthetic reactions in most cells.<sup>16</sup> The pathway converts three molecules of glucose into two molecules of fructose 6-phosphate, one molecule of glyceraldehyde 3-phosphate, and three molecules of carbon dioxide. The carbon dioxide is all derived from the C-1 of the hexose substrate, and no C-1 from this original hexose appears in the final products of the phosphogluconate pathway. A schematic representation of this pathway showing the fate of each carbon is given in Figure 5. By calculating the probabilities of labeled and unlabeled glucose being incorporated into this pathway, it is possible to predict the isotopomers generated by any catabolism through this pathway. The different isotopomers and their percentage as a fraction of all molecules produced by this pathway are shown in Table III. In this treatment it is assumed that (1) the catabolic products are used for polysaccharide biosynthesis and (2) six glucose molecules produce six molecules of  $\text{CO}_2$  and five hexose units. The pyruvate acetal carbons are derived from a seventh molecule of glucose.

The isotopomer distribution predicts that the overall extent of labeling within the hexose units will be 18.3% and that each individual position will be enriched to a level of 18.3%. However,

**Table III.** Predicted Isotopomers from the Phosphogluconate Pathway with 20% [ $^{13}\text{C}_6$ ]Glucose

predicted isotopomer	percentage
1-2-3-4-5-6	58.2
1-2-3*-4-5-6	4.9
1*-2*-3-4-5-6	4.9
1*-2*-3*-4-5-6	4.9
1-2-3-4*-5*-6*	4.9
1-2-3*-4*-5*-6*	4.9
1*-2*-3-4*-5*-6*	4.9
1*-2*-3*-4*-5*-6*	3.6

**Table IV.** Percentages of Catabolized Substrate Calculated for the Cross Peaks in Figure 4<sup>a</sup>

cross peak	catabolism	cross peak	catabolism
$\text{C}_{12}^2$	36	$\text{C}_{34}^3$	24
$\text{C}_{23}^2$	33	$\text{C}_{45}^4$	43

<sup>a</sup> Each value is the average of 10 measurements.

**Table V.** Level of Glucose Catabolism Calculated by Comparing the Ratio of the C-1 and C-2 Resonances from Each Residue of the K3 Serotype Polysaccharide

residue	catabolism, %	residue	catabolism, %
$\alpha$ -galA (A)	24	$\alpha$ -man (C)	29
$\alpha$ -man (B)	34	$\beta$ -gal (D)	38

it is predicted that the proportion of  $^{13}\text{C}$ - $^{13}\text{C}$  pairs is only 8.5% for C-2-C-3, and for C-3-C-4, but it is 18.3% for C-1-C-2, C-4-C-5, and C-5-C-6; thus all the biosynthetic information is contained in the distribution of these pairs of isotopomers. From these predictions (Table III) it is possible to calculate the contribution that each isotopomer will make to each cross peak. We combined these individual components to arrive at the multiplet patterns for a hypothetical situation where all glucose is metabolized through the phosphogluconate pathway (Figure 6).

It is noticeable that these constructions predict that the effect of substrate catabolism is reflected only in the  $\text{C}_{12}^2$ ,  $\text{C}_{23}^2$ ,  $\text{C}_{34}^3$  and  $\text{C}_{45}^4$  cross peaks. This is in excellent agreement with the observed cross peaks; additional multiplet components are observed only at these four correlations (see Figure 4). It is now possible to estimate the extent of catabolism via the phosphogluconate pathway by comparing the predicted cross peaks with the observed cross peaks. Taking the  $\text{C}_{12}^2$  cross peak of  $\beta$ -D-galactose (D) residue as an example, the observed ratio of the double doublet ( $\text{C}_3$ ) to doublet ( $\text{C}_2$ ) multiplets is 20:7. This was confirmed by computer simulation of the multiplet pattern, while the predicted ratio of  $\text{C}_3:\text{C}_2$  is 1:2.3. Subtracting the contribution of the catabolic products to the double doublet, we arrive at a value of 31% for catabolized substrate. The results for this analysis are summarized below, the values given being the averages of 10 measurements, i.e., 5 residues, with 2 cross peaks in each (Table IV). Note that the predicted level of  $^{13}\text{C}$  enrichment for the pair of carbons that give rise to the  $\text{C}_{34}^3$  cross-peak is approximately half of that for the other cross peaks. This is reflected in a much lower signal-to-noise ratio in the final spectrum, leading to a much larger error in the measured intensities of the cross peaks. These results clearly show that a significant proportion of the substrate is catabolized through the phosphogluconate pathway prior to incorporation into the polysaccharide.

**Labeling with [ $2\text{-}^{13}\text{C}$ ]Glucose.** A study of the phosphogluconate pathway (Figure 5) shows that the C-2 of the original hexose moiety appears in the catabolic products at C-1 and C-3 but not at C-2. We used this fact to confirm the results in the COSY spectrum by biosynthetically enriching the polysaccharide with [ $2\text{-}^{13}\text{C}$ ]glucose. We predicted that the resulting spectrum should show enhancement of C-1 and C-3 signals if there is significant catabolism through the phosphogluconate pathway. Any enhancement of the C-2 signals will be purely as a result of direct incorporation of the hexose into the polysaccharide. Furthermore, the ratios of the C-1 to C-3 peak intensities should be approximately 2:1. We can also predict a small enhancement of the C-5

(7) Fosdick, L. S.; Dodds, A. F. *Arch. Biochem.* **1945**, *6*, 1-8.

(8) Sprenger, G. A.; Lengler, J. W. *J. Gen. Microbiol.* **1988**, *134*, 1635-1644.

(9) Kelker, N. E.; Simkins, R. A.; Anderson, R. L. *J. Biol. Chem.* **1972**, *247*, 1479-1483.

(10) Simpson, F. J.; Wolin, M. J.; Wood, W. A. *J. Biol. Chem.* **1958**, *230*, 457-472.

(11) St. Martin, E. J.; Mortlock, R. P. *J. Bacteriol.* **1980**, *141*, 1157-1162.

(12) Chartnertzky, W. T.; Mortlock, R. P. *J. Bacteriol.* **1974**, *119*, 162-169.

(13) Anderson, R. L.; Wood, W. A. *J. Biol. Chem.* **1962**, *237*, 296-303.

(14) De Ley, J. *Enzymologia* **1957**, *18*, 33-46.

(15) Utter, M. F. *Ann. Rev. Biochem.* **1958**, *27*, 245-284.

(16) Lehninger, A. L. *Biochemistry*, 2nd ed.; Worth: New York, 1975.

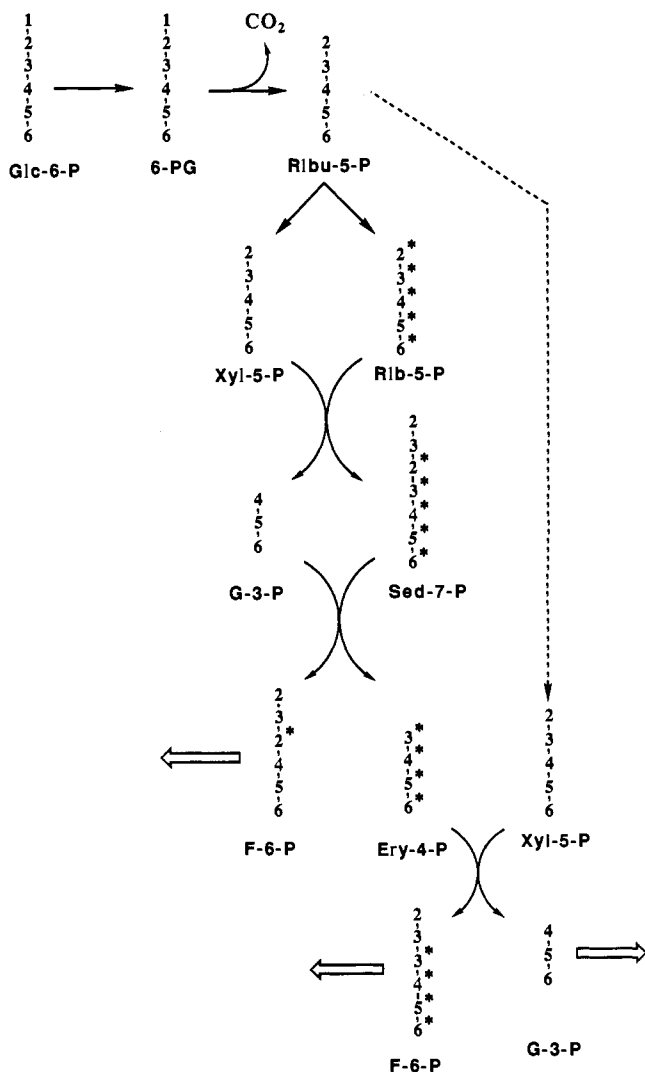


**Figure 5.** Schematic representation of the phosphogluconate pathway showing the fate of each carbon that enters this cycle. Key: Glc-6-P, glucose 6-phosphate; 6-PG, 6-phosphogluconate; Ribu-5-P, ribulose 5-phosphate; Xyl-5-P, xylulose 5-phosphate; Rib-5-P, ribose 5-phosphate; G-3-P, glyceraldehyde 3-phosphate; Sed-7-P, sedoheptulose 7-phosphate; F-6-P, fructose 6-phosphate; Ery-4-P, erythrose 4-phosphate.

resonances based on the observations of labeling with  $[1-^{13}\text{C}]$ -glucose. To investigate these predictions, we prepared a sample grown with  $\alpha\text{-D-[2-}^{13}\text{C}]$ glucose as the carbon source and an unlabeled control. The resulting spectra are shown in Figure 7.

The spectra clearly show enhancement of the predicted signals at the C-1, C-2, and C-3 resonances. The extent of substrate catabolism is calculated by comparing the C-1 to C-2 peak ratios in the control and labeled spectra. The C-2 intensities represent 20% of all molecules incorporated directly into the polysaccharide while the C-1 intensities represent 15% of all molecules metabolized through the phosphogluconate pathway. The results are presented in Table V and, within experimental error, agree with the independent COSY experiment.

### Discussion

All the spectra discussed here were obtained on whole cultures under physiological conditions and without prior isolation of the polysaccharide. This simple experimental protocol, which avoids the need for isolation and purification, is a result of the large amount of extracellular polysaccharide produced by the bacterium when grown on a nitrogen-limiting medium. Background signals are, with the exception of free glucose, too small to interfere.

NMR spectroscopy has often been used to investigate the biosynthesis and metabolism of cellular components. However, the general approach with  $^{13}\text{C}$  NMR spectroscopy has involved

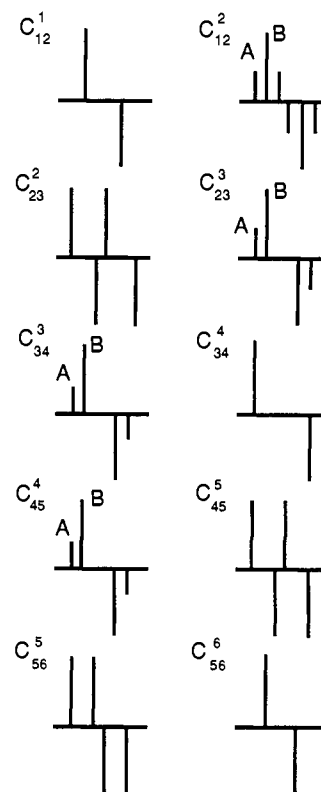


**Figure 6.** Predicted COSY multiplet patterns for the K3 serotype polysaccharide synthesized from hexose produced solely via the phosphogluconate pathway for a culture grown on 20%  $[\text{U-98\%}-^{13}\text{C}_6]$ glucose. The predicted ratio of A:B is 1:2.3 for  $\text{C}_{12}^2$  and  $\text{C}_{45}^4$  and 1:2.7 for  $\text{C}_{23}^3$  and  $\text{C}_{34}^3$ .

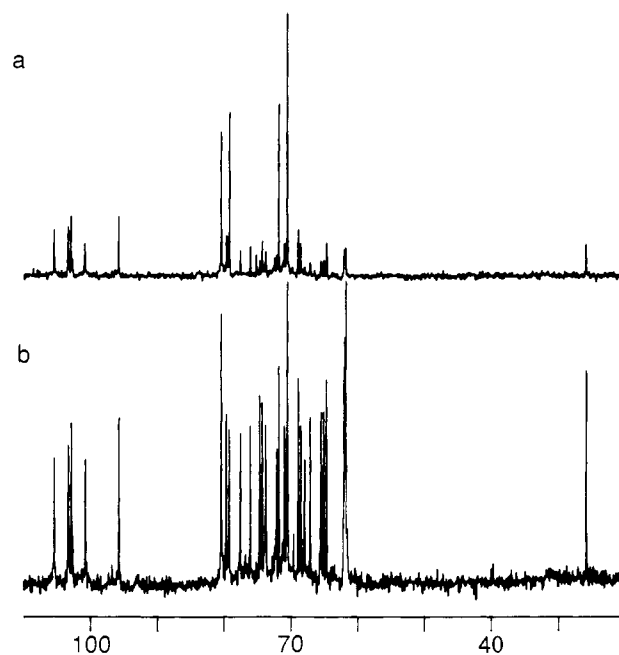


**Figure 7.** One-dimensional spectra of the *Klebsiella* K3 serotype polysaccharide from cultures grown on (a)  $[2-^{13}\text{C}]$ glucose, 60000 transients, and (b)  $[\text{U-14\%}-^{13}\text{C}_6]$ glucose, 40000 transients. Acquisition parameters are the same as Figure 1.

the use of purely one-dimensional techniques to study the incorporation of a label into a specific site. The labeling studies outlined above have extended this approach to prepare samples for two-dimensional spectroscopy and have demonstrated how  $^{13}\text{C}$ -COSY spectroscopy can be used to study the biosynthesis of bacterial polysaccharides. Clearly this is a far more exciting prospect as the  $^{13}\text{C}$ -COSY contains a wealth of information re-

garding biosynthetic and catabolic pathways in addition to providing a complete assignment of the  $^{13}\text{C}$  spectrum. An obvious extension of this technique would be to use heteronuclear shift correlation to trace the biosynthetic fate of, say,  $^{15}\text{N}$ - $^{13}\text{C}$ ,  $^{13}\text{C}$ - $^{31}\text{P}$ , or  $^{13}\text{C}$ - $^2\text{H}$  pairs.

A biosynthetic labeling strategy must always be carefully planned, and especially so when it is used to prepare samples for  $^{13}\text{C}$  NMR spectroscopy. High concentrations of  $^{13}\text{C}$  label may, in the absence of a  $^{13}\text{C}$  decoupling technique, lead to more confused and complex spectra. This is important when the natural abundance spectrum is already crowded. The exact level and distribution of labeling used will depend upon the nature of the information required and the corresponding type of experiment to be performed. To establish the patterns of spin connectivities,  $^{13}\text{C}$ -COSY techniques require that many of the spins are coupled, and this demands a level of  $^{13}\text{C}$  enrichment high enough to ensure that there are many pairs of  $^{13}\text{C}$ - $^{13}\text{C}$  throughout the molecule. On the other hand, this pattern of labeling would only serve to confuse other experiments. For example, in inverse detected heteronuclear chemical shift correlation experiments<sup>17</sup> the resulting correlations would all appear as doublets in the  $f_1$  dimension; in this case it would be more appropriate to enrich the sample at a uniform but low level and so avoid the confusion arising from  $^{13}\text{C}$ - $^{13}\text{C}$  couplings.

The information contained in the cross-peak correlations is dependent on the distribution of  $^{13}\text{C}$ - $^{13}\text{C}$  pairs throughout the molecule. Clearly for this experiment to work, the extent of labeling must be high enough to produce a detectable level of  $^{13}\text{C}$ - $^{13}\text{C}$  couplings. However, it is important to realize that in using  $^{13}\text{C}$ -COSY, 100% labeling is almost as useless as no labeling at all. The success of our approach depends upon labeled carbon pairs combining with unlabeled carbons. Without the unlabeled material all the cross peaks would appear as simple double doublets and there would be no information regarding the catabolic activity.

It is also necessary to choose carefully the experiment to be performed. For example,  $^{13}\text{C}$ -COSY appears to be preferred to the standard INADEQUATE sequence for the following reasons: first, the INADEQUATE experiment contains a fixed delay of  $1/2J$ , which leads to dramatic loss of signal in rapidly relaxing molecules such as large polysaccharides or proteins; second, correlations in INADEQUATE spectra, although essentially containing the same information as the COSY technique, have unpredictable intensities; finally, in the INADEQUATE experiment if three spins A, M, and X are mutually coupled, there will be correlations between A and X as well as correlations between A and M and M and X. While this phenomenon has been exploited in previous biosynthetic studies,<sup>1</sup> if the spectrum is already crowded it may prove a hindrance to spectral interpretation by further crowding the spectrum. The triple-quantum-filtered INADEQUATE<sup>1</sup> will give fewer cross peaks by filtering out any isotopomers containing only two coupled carbons.

The detailed patterns of the multiplets in the cross peaks of the spectrum are diagnostic of the pathways involved in the polysaccharide biosynthesis. Furthermore, the cross peaks reflect both the nature and the extent of each catabolic and biosynthetic pathway involved in the eventual production of the polysaccharide. This is in distinct contrast to experiments with specifically labeled substrates such as  $[1-^{13}\text{C}]$ glucose. This experiment (Figure 1) showed no evidence of catabolic pathways other than the glycolytic pathway as an alternative to direct incorporation of the hexose into the polysaccharide. In particular there was no evidence for the phosphogluconate pathway due to the loss of the C-1 label to carbon dioxide. This experiment clearly demonstrates the danger of interpreting single-labeling experiments in isolation. Further, detailed analysis of biosynthetic pathways by one-di-

mensional techniques is all too often not possible even if a complete spectral assignment has already been made.

These results clearly demonstrate that the major biosynthetic pathway for polysaccharide production in *Klebsiella rhinoscleromatis* proceeds via intact incorporation of the hexose unit into the polysaccharide. However, it is clear that a substantial proportion of the glucose substrate is catabolized prior to incorporation into the polysaccharide. This catabolism proceeds almost exclusively via the phosphogluconate pathway, and approximately 30% of all glucose is catabolized through this pathway prior to incorporation into the polysaccharide.

The conversion of the hexose units from glucose to mannose and galactose for polysaccharide biosynthesis proceeds via a series of enzymic reactions.<sup>18</sup> These reactions occur following activation of the monosaccharide by conversion into mono- or diphosphoric esters of deoxynucleotides, and they retain the hexose carbon skeleton established prior to activation. So the fact we observe similar isotopomer distributions for all the hexoses in the polysaccharide confirms that these structural modifications all take place directly from a hexose pool and that the phosphogluconate pathway returns newly synthesized hexose back into the same pool.

### Conclusions

We have shown that  $^{13}\text{C}$ -COSY spectroscopy is a new and very powerful tool for the biosynthetic studies of complex molecules; the approach has obvious potential for spin pairs other than  $^{13}\text{C}$ - $^{13}\text{C}$  illustrated here.

### Experimental Section

**Growth Media.** Brain heart infusion (BHI) agar and broth and bacteriological agar were obtained from Oxoid Ltd. as dehydrated powders and were reconstituted and sterilized before use.

Agar plates (9-mm diameter) were prepared with the following medium (25 mL each): yeast extract (Oxoid Ltd.) (2 g), magnesium sulfate (anhydrous) (0.25 g), sodium chloride (2 g), potassium sulfate (1 g), agar (15 g), and glucose (4 g) dissolved in 1 L of distilled water.

For biosynthetic labeling mixtures of  $^{13}\text{C}$ -labeled glucose and unlabeled glucose were used in the following amounts per 125 mL of growth medium: (1)  $\alpha$ -D- $[1-^{13}\text{C}]$ glucose (100 mg) and  $\alpha$ -D-glucose (400 mg); (2)  $\alpha$ -D- $[^{13}\text{C}_6]$ glucose (100 mg) and  $\alpha$ -D-glucose (400 mg); (3)  $\alpha$ -D- $[2-^{13}\text{C}]$ glucose (100 mg) and  $\alpha$ -D-glucose (400 mg).  $\alpha$ -D- $[^{13}\text{C}_6]$ Glucose (98.2 at.%),  $\alpha$ -D- $[^{13}\text{C}_6]$ glucose (14 at.%), and  $\alpha$ -D- $[1-^{13}\text{C}]$ glucose (99 at.%) were obtained from M.S.D. Isotopes.  $\alpha$ -D- $[2-^{13}\text{C}]$ Glucose (99 at.%) was a gift from Dr. Anthony Serianni, University of Notre Dame.

**Phosphate-Buffered Saline.** Phosphate-buffered saline at pH 7 was prepared from disodium hydrogen orthophosphate ( $\text{Na}_2\text{HPO}_4 \cdot 2\text{H}_2\text{O}$ , 0.2 M, 305 mL), sodium dihydrogen orthophosphate ( $\text{NaH}_2\text{PO}_4 \cdot 2\text{H}_2\text{O}$ , 0.2 M, 195 mL), and sodium chloride (11.3 g) made up to 1 L with distilled water.

**Sample Preparation.** A culture of *Klebsiella rhinoscleromatis* (ATCC 13884, NCTC 5046) capsular serotype K3, was obtained from Dr. I. Ørskov, Copenhagen. The bacteria were stored on BHI agar slants at 4 °C and recultured at monthly intervals from an unopened vial. The bacteria were grown in BHI broth ( $2 \times 9$  mL, 30 h at 32 °C). The resulting suspension was used to inoculate five glucose agar plates (0.2 mL each). Following incubation (48 h at 32 °C) the culture was harvested and resuspended in  $\text{D}_2\text{O}$ /PBS (1.5 mL:2.5 mL).

**NMR Details.** All spectra were recorded on a Bruker AM 400 spectrometer operating at 100 MHz carbon (9.4 T). One-dimensional spectra were recorded with a 10-mm VSP probe, using composite pulse decoupling (WALTZ-16)<sup>19</sup> in all cases and two-dimensional spectra with a 5-mm carbon/proton dual probe. Detailed parameters are presented with each spectrum.

**Acknowledgment.** We thank Dr. Andy Crawford for his comments and help with the computer simulations, Dr. Anthony Serianni for his generous gift of specifically labeled sugars, and the SERC and Unilever Research for a CASE Studentship to D.N.M.J.

(17) Cavanagh, J.; Hunter, C. A.; Jones, D. N. M.; Keeler, J.; Sanders, J. K. M. *Magn. Reson. Chem.* **1988**, *26*, 867-875.

(18) Shibaev, V. N. *Adv. Carbohydr. Chem. Biochem.* **1986**, *44*, 277-339.  
(19) Shaka, A. J.; Keeler, J.; Freeman, R. J. *Magn. Reson.* **1983**, *53*, 313-340.